

Article

Research on Estimation Method of Fuel Cell Health State Based on Lumped Parameter Model

Xueshuang Ren ¹, Xin Zhang ^{1,*}, Teng Teng ¹ and Congxin Li ²

¹ Institute of Electrical and Mechanical, Beijing Jiaotong University, Beijing 100044, China; 18121399@bjtu.edu.cn (X.R.); 18116041@bjtu.edu.cn (T.T.)

² National New Energy Vehicle Technology Innovation Center, Beijing 100044, China; licongxin@nevc.com.cn

* Correspondence: xinzhang@bjtu.edu.cn; Tel.: +86-132-693-280-09

Received: 31 October 2020; Accepted: 2 December 2020; Published: 4 December 2020



Abstract: The increasingly serious environmental pollution and the shortage of social energy have promoted the rapid development of fuel cell vehicles. The major factor which limits the commercialization of fuel cell vehicles is durability. Accurately estimating the state and parameters of a fuel cell is critical to extending the life of the fuel cell. To address this challenge, we extended a proton exchange membrane fuel cell (PEMFC) lumped parameter model and incorporated new algorithms that are essential to estimate the health of the fuel cell in a range-extended fuel cell car. The unscented Kalman filter (UKF) algorithm has been used to estimate the ohmic internal resistance of the fuel cell in real time. By using the unscented transformation (UT) method, the linearization of the nonlinear state equation is avoided, and the filtering accuracy is improved without increasing the complexity of the system. By comparing simulation and experimental results, the feasibility and accuracy of the algorithm in this paper are further verified. This method has high estimation accuracy and is suitable for an embedded system. The research of this method is an important basis for improving the control strategy of fuel cell vehicles. Reasonable use of fuel cells can extend battery life, and this method is of great significance to the commercialization of fuel cell vehicles.

Keywords: proton exchange membrane fuel cell; lumped parameter model; unscented Kalman filtering; unscented transformation; ohm internal resistance; performance degradation

1. Introduction

With the increasing consumption of energy in the world, the associated environmental problems have become more and more serious. In order to solve the problem of energy shortage and environmental pollution, new energy vehicles have gradually taken center stage. The fuel cell vehicles use clean energy, which can achieve pollution-free operation and zero emissions. Meanwhile, fuel cell vehicles have longer driving distance and higher power density and are more powerful than their all-electric competitors. This means fuel cell vehicles have very broad development and application prospects in transportation. Proton exchange membrane fuel cell (PEMFC) is one of the most promising new power generation devices [1]. Due to its characteristics of environmental friendliness and abundant resources, it has been widely used in transportation and other fields [2,3]. However, the two most important factors limiting the commercialization of fuel cell vehicles are price and durability, which directly determine the competitiveness of future products. Therefore, the accurate estimation of fuel cell health is very important for the rational use of fuel cells.

At present, there are many ways to estimate fuel cell state of health. Particle filtering [4] is a method based on Monte Carlo simulation, which is similar to the Bayesian filtering method. This method is not limited by system models and noise. Particle sets can achieve recursive propagation through the Bayesian criterion. This method can combine the unobservable state with the physical model,

and can consider the uncertainty related to the prediction [5,6], but does not consider the variable load conditions. The degradation mechanism model fully considers the three most important aging phenomena during the operation of proton exchange membrane fuel cells: ohmic loss, reactivity loss and mass transfer loss of reactants [7,8]. By solving the implicit Butler–Volmer equation, the activation loss value under different load curves can be accurately obtained, which is robust and reliable. However, the degradation mechanism model needs to consider the internal physical and chemical characteristics of the fuel cell, so it is difficult to establish an accurate aging mechanism model [9]. ESN [10] is a new type of recursive neural network, which consists of an input layer, a reserve pool and an output layer. The reserve pool is a sparse network with multiple neurons [11]. The disadvantage of this method is that too many parameters are difficult to adjust and filtered data must be used [12]. Transfinite learning machine [13] is a new single hidden layer feedforward neural network (SLFN). The connection weights between the input layer and the hidden layer and the thresholds of the hidden layer neurons are randomly generated [14], and no iteration is required during the training process; the learning efficiency is high, and the generalization performance is strong [15]. The data-driven method is to obtain a large amount of offline battery data by charging and discharging the battery and establishing a model in which the battery voltage, current, temperature and other data have a mapping relationship with the battery. This method does not need to consider the characteristics and details of the internal chemical reaction of the battery [16,17]. Relevance vector machine [18] can provide probabilistic forecast results and can realize parameters automatically set and artificial selection of kernel function. Its high sparsity can effectively reduce the amount of calculation. A non-nuclear list of extension design matrix can be obtained from the fuel cell degradation data linear and nonlinear characteristics [19]. The neural network method can estimate the battery parameters. This method has a strong dependence on the data set, and the algorithm's antisturbance ability is insufficient [20]. The Gaussian process state-space model [21] can obtain the uncertainty by estimating the distribution, thereby obtaining the accuracy of the inference. This method is only used under the condition of constant current fuel cell data and does not consider the change of internal parameters [22]. The above methods of estimating the health status of the fuel cell each have their own advantages and disadvantages, and a researcher can choose the appropriate method according to their actual situation.

In this paper, a proton exchange membrane fuel cell model is established, and the unscented Kalman filter (UKF) algorithm is used to estimate the ohmic resistance of the cell. The results of the study show that the ohmic resistance of the fuel cell slowly increases during use, and the sharp increase or decrease of the current will cause the ohmic resistance to increase rapidly, so this method provides an important basis for the rational use of fuel cells. Figure 1 shows the research content of this article.

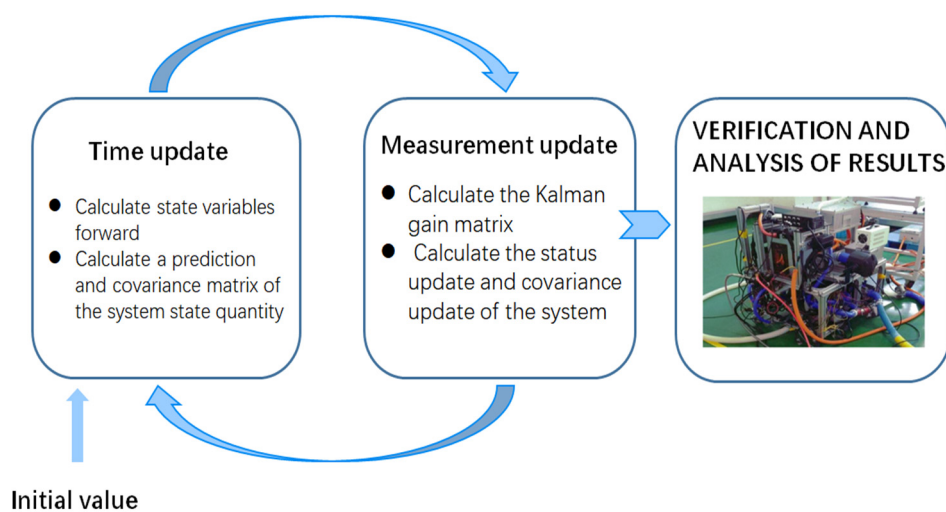


Figure 1. The research content of this article.

2. Materials and Methods

2.1. Fuel Cell Model

The fuel cell model can accurately describe the internal operating characteristics of the cell [23], and the lumped parameter model is not affected by the space. This article will establish a lumped parameter model of a PEMFC. In order to simplify the working process of fuel cells, it is necessary to make assumptions about the working process of fuel cells: (1) the internal temperature of the battery is uniform and maintained at 348.15 K; (2) the internal humidity of the battery is even, and the humidification degree is always 100%; (3) the reaction gas inside the battery is an ideal gas, which conforms to the law of ideal gas; (4) regardless of the differences between the individual cells of the model, the model is a one-dimensional lumped parameter model. Figure 2 is the working principle diagram of the fuel cell.

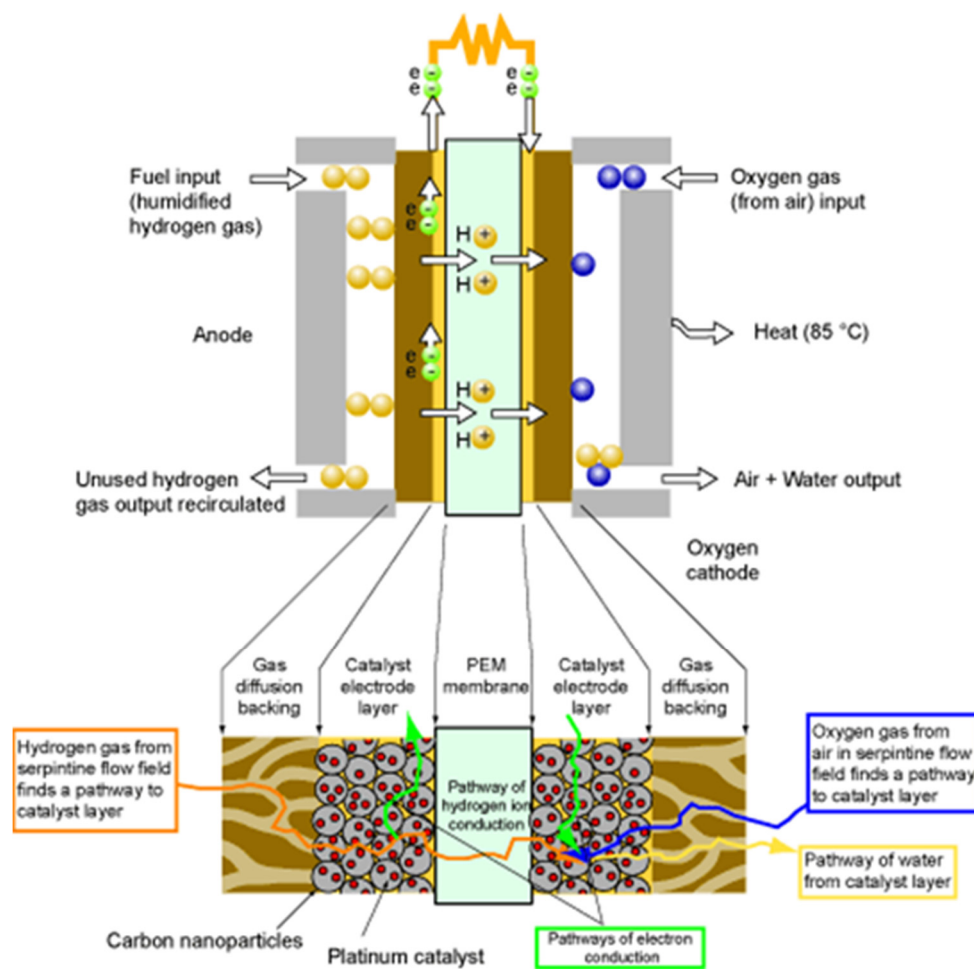


Figure 2. Working principle diagram of proton exchange membrane fuel cell (PEMFC).

During the use of the fuel cell, electrons will accumulate on the battery surface and ions will accumulate on the electrolyte surface, so that there will be a voltage between them, which is equivalent to an equivalent capacitance C (F) [24]; this paper takes 3F. Figure 3 is the working principle diagram of the fuel cell [25].

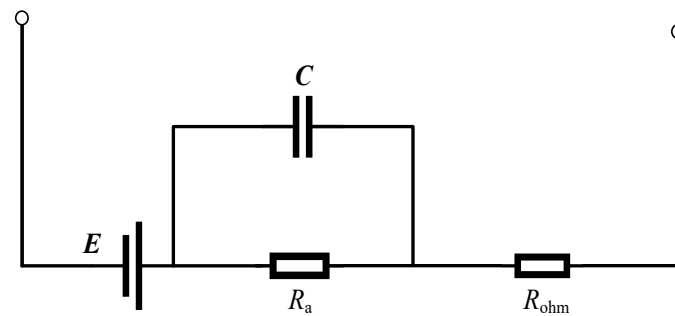


Figure 3. Equivalent circuit model of PEMFC.

The irreversible loss of the battery called the polarization overpotential is mainly caused by the activated polarization, the ohmic polarization and the concentration polarization [26].

The output voltage of proton exchange membrane fuel cell is determined as follows [27]:

$$V_{cell} = E_{Nernst} - \eta_{act} - \eta_{\Omega} - \eta_{con} \quad (1)$$

where E_{Nernst} is the thermodynamic electromotive force, a simplified expression of which can be obtained from the equation of hydrogen and oxygen fuel cell [28]:

$$E_{Nernst} = 1.229 - 8.5 \times 10^{-4} \times (T - 298.15) + 4.308 \times 10^{-5} \times T \times (\ln p_{H_2} + 1/2 \ln p_{O_2}) \quad (2)$$

where T is the working temperature of PEMFC, p_{H_2} is the partial pressure of hydrogen and p_{O_2} is the partial pressure of oxygen.

Here, η_{act} is the activation overvoltage, which is used to activate the electrochemical reaction, and is caused by the polarization of the battery. The empirical model can be obtained from the literature [29]:

$$\eta_{act} = \xi_1 + \xi_2 T + \xi_3 \ln(C_{O_2}) + \xi_4 T \ln i \quad (3)$$

where ξ_1 , ξ_2 , ξ_3 and ξ_4 are empirical values related to kinetics, thermodynamics and electrochemistry. Generally applicable values are selected in this paper [30]: $\xi_1 = -0.9514$, $\xi_2 = 0.0312$, $\xi_3 = 7.4 \times 10^{-5}$ and $\xi_4 = 1.87 \times 10^{-4}$. i is the fuel cell current (A) and C_{O_2} is the oxygen concentration at the cathode gas interface (mol/cm³) and is expressed as follows:

$$C_{O_2} = \frac{p_{O_2}}{5.08 \times 10^6 \exp(-498/T)} \quad (4)$$

where η_{Ω} is ohmic overvoltage, which is generated by the impedance received during the movement of protons in electrolyte and electrons in electrode [31]. Ohmic overvoltage conforms to Ohm's law, and its expression is

$$\eta_{\Omega} = iR_{ohm} = i(R_m + R_c) \quad (5)$$

where R_{ohm} is the ohmic internal resistance of the fuel cell, R_c is the impedance that obstructs the passage of electrons through the membrane and R_m is the impedance of the proton exchange membrane and is expressed as follows [32]:

$$R_m = \frac{r_M l}{A} \quad (6)$$

where l is the thickness of the membrane (cm), A is the area of the membrane (cm²) and r_M is the resistivity of the proton exchange membrane.

Here, η_{con} is concentration difference overvoltage, which is the concentration difference overvoltage caused by insufficient supply of reaction gas in the condition of high current density, and its expression is as follows:

$$\eta_{con} = -B \ln\left(1 - \frac{J}{J_{max}}\right) \quad (7)$$

where B is constant and is related to the working state of the battery, J is the actual current density of the battery (A/cm^2) and J_{max} is the maximum current density of the battery and has a value of $2 A/cm^2$ according to the vehicle parameters.

The dynamic characteristics of electrochemical reaction and reactant transport in the stack have the greatest influence on the output dynamic characteristics of the fuel cell. The total output voltage of PEMFC can be expressed as

$$V_0 = E - V_{act} - V_{con} - R_{ohm}I \quad (8)$$

The fuel cell current I , hydrogen partial pressure p_{H_2} and oxygen partial pressure p_{O_2} of the fuel cell are selected as input variables, and the output voltage V_0 of the fuel cell is selected as the output variable. The fuel cell parameter values are shown in Table 1.

Table 1. The fuel cell parameter values.

Parameter	Value	Unit
T	348.15	K
C	3	F
ξ_1	-0.9514	/
ξ_2	0.0312	/
ξ_3	7.4×10^{-5}	/
ξ_4	1.87×10^{-4}	/
A	232	cm^2
J_{max}	2	A/cm^2

2.2. Unscented Kalman Filter Algorithm to Estimate the Fuel Cell State

2.2.1. Model Discretization

Unscented Kalman filter is a nonlinear filtering method. Instead of linearizing nonlinear functions, the Kalman linear filtering framework is used. This framework chooses nearby sampling points and then uses the Gaussian density approximation of these sampling points to approximate the probability density function instead of approximating the nonlinear function [33]. Therefore, this method has high computational accuracy for the statistics of nonlinear distribution, and it can solve the problem of low estimation accuracy and poor stability of the extended Kalman filter algorithm.

The PEMFC model can be obtained by discretization [34]:

$$\begin{bmatrix} U_{1,k+1} \\ R_{ohm,k+1} \end{bmatrix} = \begin{bmatrix} \exp(-T/r_1/c) & 0 \\ 0 & 1 \end{bmatrix} \begin{bmatrix} U_{1,k} \\ R_{ohm,k} \end{bmatrix} + \begin{bmatrix} r_1[1 - \exp(-T/r_1/c)] \\ 0 \end{bmatrix} i_k + w_k \quad (9)$$

$$U_k = E_k - U_{1,k} - U_{2,k} - i_k R_O + v_k \quad (10)$$

where i is the current value control variable; U_k is the voltage value of the fuel cell terminal, which is an observed variable; E_k is the ideal open circuit electromotive force; R_O is the theoretical internal resistance at the current moment; k is the acquisition time; w_k is the system noise; Q is the covariance; and v_k is the observation noise, and its covariance is R .

The coefficient matrix of the state-space model is

$$A = \begin{bmatrix} \exp(-T/r_1/c) & 0 \\ 0 & 1 \end{bmatrix} B = \begin{bmatrix} r_1[1 - \exp(-T/r_1/c)] \\ 0 \end{bmatrix}$$

Based on this model, this paper uses the unscented Kalman filter method to estimate the ohmic internal resistance of the fuel cell.

2.2.2. Unscented Kalman Filter Estimates the Ohmic Internal Resistance of Fuel Cells

The difference between the UKF method and EKF method is that the nonlinear equation is not linearized at the estimated point. Instead, sigma point set is obtained by UT transformation [35], and the corresponding weight is calculated to calculate the statistical characteristics of the nonlinear function. The specific steps to estimate the ohmic internal resistance of the fuel cell using UKF are as follows:

- (1) Calculate sigma points, and the number of sampling points is $2n+1$:

$$\begin{cases} X^{(0)} = \bar{X}, i = 0 \\ X^{(i)} = \bar{X} + \left(\sqrt{(n+\lambda)P}\right)_i, i = 1 \sim n \\ X^{(i)} = \bar{X} - \left(\sqrt{(n+\lambda)P}\right)_i, i = n+1 \sim 2n \end{cases} \quad (11)$$

where n represents the dimension of state, the \bar{X} represents the average value of the input variable X and the $\left(\sqrt{(n+\lambda)P}\right)_i$ represents the i column of the matrix.

- (2) Calculate the weight of sigma points:

$$\begin{cases} \omega_m^{(0)} = \frac{\lambda}{n+\lambda} \\ \omega_c^{(0)} = \frac{\lambda}{n+\lambda} + (1 - \alpha^2 + \beta) \\ \omega_m^{(i)} = \omega_c^{(i)} = \frac{\lambda}{2(n+\lambda)}, i = 1 - 2n \end{cases} \quad (12)$$

where λ represents the scaling parameter, which can reduce the prediction error, and its expression is $\lambda = \alpha^2(n + \kappa) - n$; m represents the average; c represents the covariance; α represents sigma point deviation from the value of the estimated state, called the scale factor, and is in the typical range of $10^{-4} \leq \alpha \leq 1$; β represents a point distribution related to sigma, when the sigma point integration is in Gaussian distribution, where $\beta = 2$ is usually selected as the best estimation result; and κ represents the adjustment factor, ensuring that $(n + \lambda)P$ is a semipositive definite matrix.

- (3) One-step prediction of sigma point set:

$$X^{(i)}(k+1|k) = f[k, X^{(i)}(k|k)], i = 1, 2, \dots, 2n+1 \quad (13)$$

- (4) Calculate a prediction and covariance matrix of the system state quantity. Traditional Kalman filtering is to bring the state into the state equation at the last moment and calculate the state prediction only once. Unlike traditional Kalman filtering, the UKF uses a sigma point set of prediction, calculating the weighted average of the sigma point set and obtaining a one-step prediction of the system state:

$$\hat{X}(k+1|k) = \sum_{i=0}^{2n} \omega^{(i)} X^{(i)}(k+1|k) \quad (14)$$

$$P(k+1|k) = \sum_{i=0}^{2n} \omega^{(i)} [\hat{X}(k+1|k) - X^{(i)}(k+1|k)][\hat{X}(k+1|k) - X^{(i)}(k+1|k)]^T + Q \quad (15)$$

- (5) A new set of sigma points is obtained by using the unmarked transformation again on the predicted value of the above step:

$$X^{(i)}(k+1|k) = \begin{bmatrix} \hat{X}(k+1|k) \\ \hat{X}(k+1|k) + \sqrt{(n+\lambda)P(k+1|k)} \\ \hat{X}(k+1|k) - \sqrt{(n+\lambda)P(k+1|k)} \end{bmatrix} \quad (16)$$

- (6) Bring the new sigma point set into the observation equation and get a prediction of the observation:

$$Z^{(i)}(k+1|k) = h[X^{(i)}(k+1|k)] \quad (17)$$

- (7) Obtain the predicted value and covariance matrix of the observational measurement by one-step weighted summation:

$$\begin{cases} \bar{Z}(k+1|k) = \sum_{i=0}^{2n} \omega^{(i)} Z^{(i)}(k+1|k) \\ P_{Z_k Z_k} = \sum_{i=0}^{2n} \omega^{(i)} [Z^{(i)}(k+1|k) - \bar{Z}(k+1|k)] [Z^{(i)}(k+1|k) - \bar{Z}(k+1|k)]^T + R \\ P_{X_k Z_k} = \sum_{i=0}^{2n} \omega^{(i)} [X^{(i)}(k+1|k) - \bar{X}(k+1|k)] [Z^{(i)}(k+1|k) - \bar{Z}(k+1|k)]^T \end{cases} \quad (18)$$

- (8) Calculate the Kalman gain matrix:

$$K(k+1|k) = P_{X_k Z_k} P_{Z_k Z_k}^{-1} \quad (19)$$

- (9) Calculate the status update and covariance update of the system:

$$\begin{aligned} \hat{X}(k+1|k+1) &= \hat{X}(k+1|k) + K(k+1) [Z(k+1) - \hat{Z}(k+1|k)] \\ P(k+1|k+1) &= P(k+1|k) - K(k+1) P_{Z_k Z_k} K^T(k+1) \end{aligned} \quad (20)$$

The steps of UKF algorithm are shown above. It can be found that this method does not need to do Taylor expansion, does not increase the calculation amount and does not need to approximate the first order of n , which improves the accuracy and is a better estimation method.

3. Results

In order to verify the accuracy of the above algorithms in estimating the state of the fuel cell, the fuel cell test system shown in Figure 4 is used in this paper, which is mainly composed of the fuel cell battery, the gas supply subsystem, the humidification subsystem, the auxiliary heat dissipation subsystem, the energy management subsystem and the data acquisition and control subsystem. The fuel cell data were substituted into the MATLAB program prepared by the UKF algorithm. The current resolution of the test bench is 0.01 A, the voltage accuracy is 0.1% FS+5 dgt, the voltage resolution is 0.01 V, the ambient temperature is -10 – 40 °C, the power range is 30–60 kW, the cooling water inlet temperature is 7 °C, the return water temperature is 12 °C, the cooling water inlet pressure is controlled at 3–4 barg, the backwater pressure is 2–3 barg and the water flow rate is 20,000 kg/h. In addition, it has functions such as an emergency stop switch machine three-color operation status indicator and a sound alarm. The rated power of the fuel cell is 30 kW, which is the same as the working process hypothesis of the fuel cell model. The internal temperature of the battery is constant at 348.15 K, and the internal humidity of the battery is constant at 100%.

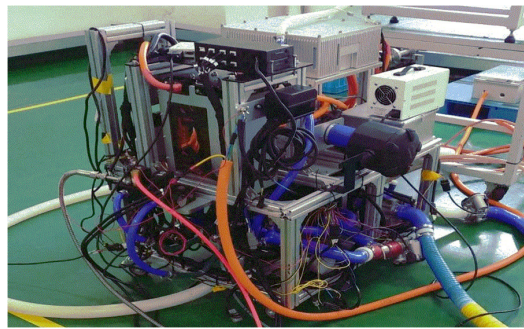


Figure 4. Test equipment.

The loading dynamic response is shown in Figure 5. Figure 6 illustrates the fuel cell ohmic resistance in between $0.01 \sim 0.02 \Omega$. When the current changes sharply, the internal water management and thermal management problems of the fuel cell cause a large change in internal resistance. It can be found from Figure 6 that during the entire operation of the fuel cell, the ohmic internal resistance gradually increases and eventually stabilizes at 0.02Ω . Table 2 shows the rate of change of the ohmic resistance of the fuel cell, takes a fuel cell ohmic resistance value every 100 seconds, a total of 10 points, and then calculates the resistance change rate at these 10 points. It can be found from the table that between 100 and 200 s, the ohmic resistance changes from 0.01043 to 0.01576Ω , and the rate of change is 0.005322% . In the same way, at approximately 500 s, the maximum resistance is 0.01789Ω , and the rate of change reaches 0.044% . The largest change rate corresponds to the stage with the largest current fluctuation of the input working conditions. It shows that UKF has a high estimation accuracy and the algorithm is effective and feasible.

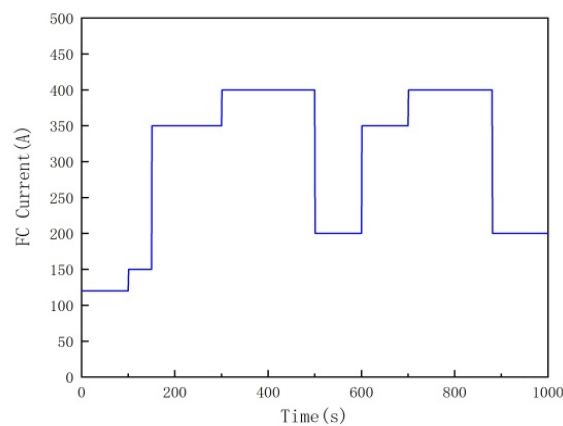


Figure 5. Loading conditions.

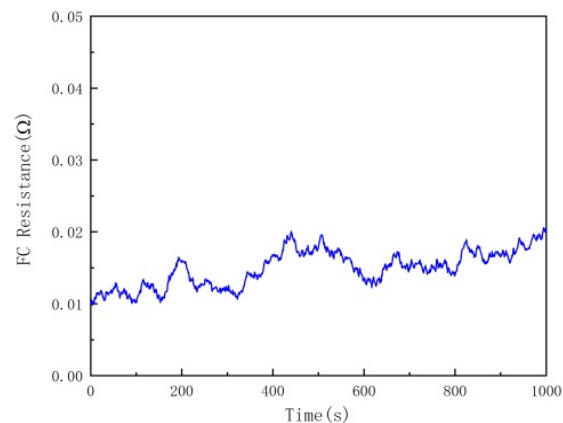


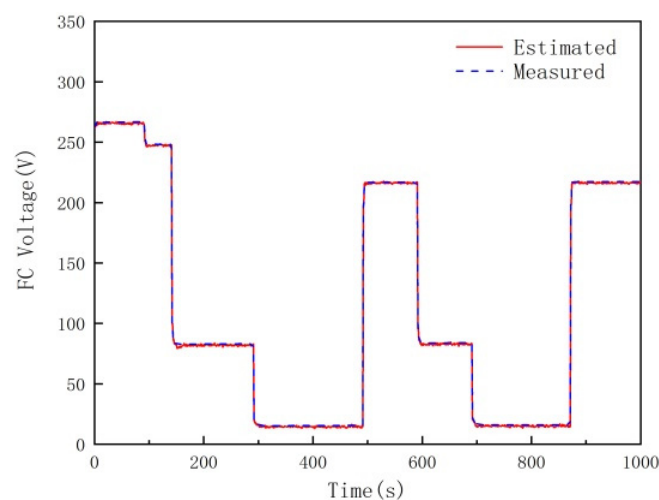
Figure 6. Ohm internal resistance.

Table 2. The rate of change of the ohmic resistance.

Time/s	Resistance/ Ω	Rate of Change/%
100	0.010434	0.000434
200	0.015756	0.005322
300	0.012132	−0.003626
400	0.016625	0.004493
500	0.017892	0.001267
600	0.013458	−0.004434
700	0.014715	0.001257
800	0.014107	−0.000608
900	0.016636	0.002529
1000	0.020643	0.004006

There are many reasons for the changes in the internal resistance of the fuel cell, such as the damage of the proton exchange membrane, the corrosion of the surface of the metal plate and the contamination of the surface of the carbon paper. The specifics need to be further studied.

Proton exchange membrane fuel cells are electrochemical products, and it is difficult to directly obtain the ohmic resistance of the battery. This article uses reverse thinking to verify it. After obtaining the ohmic resistance of the battery, we combine the circuit principle formula and working current data to estimate the battery's ohmic resistance. Then, we compare the terminal voltage obtained by inverse estimation of the estimated value with the test value. The smaller the error, the higher the estimation accuracy of this method. By comparing the test data of the fuel cell voltage and the estimated data of the algorithm, as shown in Figure 7, it can be discovered that the actual value of the fuel cell voltage differs little from the estimated value and the fluctuation is small, indicating that the estimated value of the algorithm is consistent with the actual situation. As can be seen from the error image shown in Figure 8, the error fluctuates within 2%, and the error is very small. There is no big fluctuation in the operation process. The error fluctuates greatly only in the three places where the current changes greatly, and the overall fluctuation range does not exceed -5% – 5% , indicating that UKF has high accuracy in estimating the state of the fuel cell and that it has good robustness and accuracy.

**Figure 7.** Comparison of the estimated voltage and the test voltage.

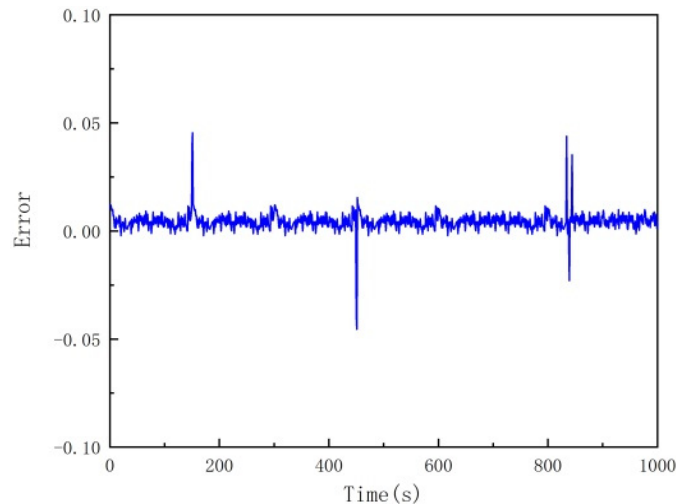


Figure 8. Error between estimated voltage and test voltage.

With the extensive application of PEMFC systems in large power fields such as buses, trams and automobiles, improving the life of fuel cell systems is an important issue. At present, the vast majority of life prediction methods are still in the experimental test stage, and the realization of online life prediction methods has not yet made a substantial breakthrough. Therefore, the study of fuel cell system online prediction method is the next research work. In addition, the prediction of the PEMFC system is mainly completed under constant operating conditions. The ohmic resistance is usually used as a health indicator to reflect the degradation degree of the fuel cell system. However, under high dynamic conditions, a single ohmic resistance does not indicate the degree of aging. Therefore, the development and verification of fuel cell aging indicators under dynamic conditions is the basis for realizing dynamic process life prediction methods and has very important research value.

4. Conclusions

Accurate estimation of fuel cell health is very important for the rational use of fuel cells. This paper studies the estimation of the health status of fuel cells. Taking ohmic internal resistance as the research object, and establishing a PEMFC lumped parameter model, the principle of UKF and the specific steps of estimating the health of the battery are introduced. According to the dynamic input conditions, the UKF algorithm is used to estimate the ohmic internal resistance. It is found that the resistance of the fuel cell gradually increases during operation. When the working conditions change sharply, the ohmic internal resistance also fluctuates sharply. Therefore, during the use of the fuel cell, frequent starting and stopping should be avoided to extend the durability of the fuel cell. Finally, through verification and comparison, it is found that the test result and the estimated result are close to the operating conditions, and the error between the two is within 2%. It can be explained that the algorithm is suitable for variable working conditions. The estimation results have high accuracy and fast speed, and it can reflect the internal changes in the working process of the fuel cell. The algorithm avoids the complexity and low accuracy of the traditional Kalman filter algorithm and proves that the UKF has good practicability. This method provides an important basis for fuel cell stack life prediction, and is conducive to the optimization of fuel cell vehicle operating parameters and control strategies, prolongs battery life and promotes fuel cell vehicle commercialization.

Author Contributions: X.R.: conceptualization, data curation, formal analysis; X.Z.: project administration, supervision; T.T.: writing—review&editing; C.L.: resources. All authors have read and agreed to the published version of the manuscript.

Funding: This research was funded by National Key Research and Development, Project-2018YFB0105401.

Conflicts of Interest: The authors declare no conflict of interest.

Nomenclature

C	Equivalent capacitance, F
T	Working temperature of PEMFC, K
p_{H_2}	The partial pressure of hydrogen, bar
p_{O_2}	The partial pressure of oxygen, bar
E_{Nernst}	Thermodynamic electromotive force, V
η_{act}	The activation overvoltage, V
η_{Ω}	The ohmic overvoltage, V
η_{con}	The concentration difference overvoltage, V
i	The fuel cell current, A
C_{O_2}	The oxygen concentration, mol/cm ³
R_c	The activated internal resistance, Ω
R_m	The impedance of PEMFC, Ω
R_{ohm}	The ohmic internal resistance, Ω
l	The thickness of the membrane, cm
A	The area of the membrane, cm ²
r_M	The resistivity of the proton exchange membrane, /
J	The actual current density, A/cm ²
J_{max}	The maximum current density, A/cm ²
k	The acquisition time, s
v_k	The observation noise, /
w_k	The system noise, /
Q	The covariance, /

References

- Laghrouche, S.; Liu, J.; Ahmed, F.S.; Harmouche, M.; Wack, M. Adaptive Second-Order Sliding Mode Observer-Based Fault Reconstruction for PEM Fuel Cell Air-Feed System. *IEEE Trans. Control. Syst. Technol.* **2015**, *23*, 1098–1109. [[CrossRef](#)]
- Li, Q.; Wang, T.; Dai, C.; Chen, W.; Ma, L. Power Management Strategy Based on Adaptive Droop Control for a Fuel Cell-Battery-Supercapacitor Hybrid Tramway. *IEEE Trans. Veh. Technol.* **2017**, *67*, 5658–5670. [[CrossRef](#)]
- Liu, J.; Li, Q.; Chen, W.; Cao, T. A discrete hidden Markov model fault diagnosis strategy based on K-means clustering dedicated to PEM fuel cell systems of tramways. *Int. J. Hydrog. Energy* **2018**, *43*, 12428–12441. [[CrossRef](#)]
- Jouin, M.; Gouriveau, R.; Hissel, D.; Pera, M.-C.; Zerhouni, N. Prognostics of Proton Exchange Membrane Fuel Cell stack in a particle filtering framework including characterization disturbances and voltage recovery. In Proceedings of the 2014 International Conference on Prognostics and Health Management, Cheney, WA, USA, 22–25 June 2014; pp. 1–6.
- Kimotho, J.K.; Meyer, T.; Sextro, W. PEM fuel cell prognostics using particle filter with model parameter adaptation. In Proceedings of the 2014 International IEEE Conference on Prognostics and Health Management (PHM), Cheney, WA, USA, 22–25 June 2014.
- Zhang, D.; Cadet, C.; Bérenguer, C.; Yousfi-Steiner, N. Some Improvements of Particle Filtering Based Prognosis for PEM Fuel Cells. *IFAC-PapersOnLine* **2016**, *49*, 162–167. [[CrossRef](#)]
- Zhou, D.; Wu, Y.; Gao, F.; Breaz, E.; Ravey, A.; Miraoui, A. Degradation Prediction of PEM Fuel Cell Stack Based on Multi-Physical Aging Model with Particle Filter Approach. *IEEE Ind. Appl. Soc. Annu. Meet.* **2016**, 1–8. [[CrossRef](#)]
- Burlatsky, S.F.; Gummalla, M.; O’Neill, J.; Atrazhev, V.V.; Varyukhin, A.N.; Dmitriev, D.V.; Erikhman, N.S. A mathematical model for predicting the life of polymer electrolyte fuel cell membranes subjected to hydration cycling. *J. Power Sources* **2012**, *215*, 135–144. [[CrossRef](#)]
- Jin, X.; Vora, A.; Hoshing, V.; Saha, T.; Shaver, G.; García, R.E.; Wasynczuk, O.; Varigonda, S. Physically-based reduced-order capacity loss model for graphite anodes in Li-ion battery cells. *J. Power Sources* **2017**, *342*, 750–761. [[CrossRef](#)]

10. Morando, S.; Jemei, S.; Hissel, D.; Gouriveau, R.; Zerhouni, N. Proton exchange membrane fuel cell ageing forecasting algorithm based on Echo State Network. *Int. J. Hydrog. Energy* **2017**, *42*, 1472–1480. [[CrossRef](#)]
11. Ben Salah, S.; Fliss, I.; Tagina, M. Echo State Network and Particle Swarm Optimization for Prognostics of a Complex System. In Proceedings of the 2017 IEEE/ACS 14th International Conference on Computer Systems and Applications (AICCSA), Hammamet, Tunisia, 30 October–3 November 2017; pp. 1027–1034.
12. Morando, S.; Jemei, S.; Gouriveau, R.; Zerhouni, N.; Hissel, D. Fuel Cells Remaining Useful Lifetime forecasting using Echo State Network. In Proceedings of the 2014 IEEE Vehicle Power and Propulsion Conference (VPPC), Coimbra, Portugal, 27–30 October 2014; pp. 1–6.
13. Javed, K.; Gouriveau, R.; Zerhouni, N.; Hissel, D. Prognostics of Proton Exchange Membrane Fuel Cells stack using an ensemble of constraints based connectionist networks. *J. Power Sources* **2016**, *324*, 745–757. [[CrossRef](#)]
14. Javed, K.; Gouriveau, R.; Zerhouni, N. Data-driven Prognostics of Proton Exchange Membrane Fuel Cell Stack with constraint based Summation-Wavelet Extreme Learning Machine. In Proceedings of the 6th International Conference on Fundamentals & Development of Fuel Cells, Toulouse, France, 3–5 February 2015.
15. Javed, K.; Gouriveau, R.; Zerhouni, N.; Hissel, D. PEM fuel cell prognostics under variable load: A data-driven ensemble with new incremental learning. In Proceedings of the 2016 International Conference on Control, Decision and Information Technologies (CoDIT), St. Julian's, Malta, 6–8 April 2016; pp. 252–257.
16. Zhenhao, S.U.; Xiaojie, L.I.; Jin, Q.N.; Wenjie, D.U.; Ning, H.A.N. Estimation method of power battery SOC based on BP artificial neural network. *Energy Storage Sci. Technol.* **2019**, *8*, 868–873.
17. Hicham, C.; Chinemerem, C.I. State of Charge and State of Health Estimation for Lithium Batteries Using Recurrent Neural Networks. *IEEE Trans. Veh. Technol.* **2017**, *66*, 8773–8783.
18. Wu, Y.; Breaz, E.; Gao, F.; Paire, D.; Miraoui, A. Nonlinear Performance Degradation Prediction of Proton Exchange Membrane Fuel Cells Using Relevance Vector Machine. *IEEE Trans. Energy Convers.* **2016**, *31*, 1570–1582. [[CrossRef](#)]
19. Wu, Y.; Breaz, E.; Gao, F.; Miraoui, A. A Modified Relevance Vector Machine for PEM Fuel-Cell Stack Aging Prediction. *IEEE Trans. Ind. Appl.* **2016**, *52*, 2573–2581. [[CrossRef](#)]
20. Li, J.; Liu, M. State-of-charge estimation of lithium-ionbatteries using composite multi-dimensional features and aneural network. *IET Power Electron.* **2019**, *12*, 1470–1478. [[CrossRef](#)]
21. Zhu, L.; Chen, J. Prognostics of PEM Fuel Cells Based on Gaussian Process State Space Models. *Energy* **2018**, *149*, 63–73. [[CrossRef](#)]
22. Ko, J.; Kleint, D.J.; Fox, D.; Haehnel, D. GP-UKF: Unscented kalman filters with Gaussian process prediction and observation models. *IEEE/RSJ Int. Conf. Intell. Robot. Syst.* **2007**, 1901–1907. [[CrossRef](#)]
23. Rahimi-Eichi, H.; Ojha, U.; Baronti, F.; Chow, M.-Y. Battery Management System: An Overview of Its Application in the Smart Grid and Electric Vehicles. *IEEE Ind. Electron. Mag.* **2013**, *7*, 4–16. [[CrossRef](#)]
24. Restrepo, C.; Konjedic, T.; Garces, A.; Calvente, J.; Giral, R. Identification of a Proton-Exchange Membrane Fuel Cell's Model Parameters by Means of an Evolution Strategy. *IEEE Trans. Ind. Inform.* **2014**, *11*, 548–559. [[CrossRef](#)]
25. Restrepo, C.; Garcia, G.; Calvente, J.; Giral, R.; Martínez-Salamero, L. Static and Dynamic Current–Voltage Modeling of a Proton Exchange Membrane Fuel Cell Using an Input–Output Diffusive Approach. *IEEE Trans. Ind. Electron.* **2015**, *63*, 1003–1015. [[CrossRef](#)]
26. Xu, L. Modeling and Simulation of Dynamic Characteristics of PEM Fuel Cells. Ph.D. Thesis, Wuhan University of Technology, Wuhan, China, 2007.
27. Baolian, Y. *Fuel Cell—Principle, Technology and Application*; Chemical Industry Press: Beijing, China, 2003.
28. O'Hayre, R.; Cha, S.; Colella, W.; Prinz, F.B. *Fuel Cell Fundamentals*; Electronics Industry Press: Beijing, China, 2007; pp. 28–40.
29. Correa, J.; Farret, F.; Canha, L.; Simoes, M. An electrochemical-based fuel-cell model suitable for electrical engineering automation approach. *IEEE Trans. Ind. Electron.* **2004**, *51*, 1103–1112. [[CrossRef](#)]
30. Mann, R.F.; Amphlett, J.C.; Hooper, M.A.; Jensen, H.M.; Peppley, B.A.; Roberge, P.R. Development and application of a generalised steady-state electrochemical model for a PEM fuel cell. *J. Power Sources* **2000**, *86*, 173–180. [[CrossRef](#)]
31. Yi, W. *Research on Hydrothermal Management System of Fuel Cell Power Plant and Demonstration of Energy Storage Scheme*; Harbin Engineering University: Harbin, China, 2015.
32. Zhan, Z.; Zhang, Y.; Xiao, J. Study on dynamic characteristics of PEMFC transmission phenomenon. *J. Wuhan Univ. Technol.* **2006**, *28*, 614–622.

33. Huang, X. *Kalman Filter Principle and Application*; China Telecom Press: Beijing, China, 2015.
34. Fu, M. *Kalman Filter Theory and Its Application in Navigation System*; Science Press: Beijing, China, 2003; pp. 8–102.
35. Grewal, M.S.A. *Kalman Filter Theory and Practice (MATLAB Edition)*, 4th ed.; Liu, Y., Chen, S., Xu, S., Eds.; Electronic Industry Press: Beijing, China, 2017.

Publisher’s Note: MDPI stays neutral with regard to jurisdictional claims in published maps and institutional affiliations.



© 2020 by the authors. Licensee MDPI, Basel, Switzerland. This article is an open access article distributed under the terms and conditions of the Creative Commons Attribution (CC BY) license (<http://creativecommons.org/licenses/by/4.0/>).